AIP | Review of Scientific Instruments

Rapid scanning fluorescence spectroscopy using an acousto-optic tunable filter

Ira Kurtz, R. Dwelle, and P. Katzka

Citation: Review of Scientific Instruments **58**, 1996 (1987); doi: 10.1063/1.1139506
View online: http://dx.doi.org/10.1063/1.1139506
View Table of Contents: http://scitation.aip.org/content/aip/journal/rsi/58/11?ver=pdfcov
Published by the AIP Publishing

Articles you may be interested in

A novel miniature spectrometer using an integrated acousto-optic tunable filter
Rev. Sci. Instrum. **65**, 3653 (1994); 10.1063/1.1145201

Infrared acousto-optic tunable filter
J. Acoust. Soc. Am. **79**, 586 (1986); 10.1121/1.393758

Acousto-optic tunable filter with controllable passband
J. Appl. Phys. **46**, 5046 (1975); 10.1063/1.321497

New noncollinear acousto-optic tunable filter using birefringence in paratellurite
Appl. Phys. Lett. **24**, 256 (1974); 10.1063/1.1655173

ELECTRONICALLY TUNABLE ACOUSTO-OPTIC FILTER
Appl. Phys. Lett. **15**, 325 (1969); 10.1063/1.1652844

This article is copyrighted as indicated in the article. Reuse of AIP content is subject to the terms at: http://scitationnew.aip.org/termsconditions. Downloaded to IP: 35.8.11.3 On: Wed, 27 Jan 2016 03:00:41

Rapid scanning fluorescence spectroscopy using an acousto-optic tunable filter

Ira Kurtz[a)]

Division of Nephrology, Department of Medicine, UCLA School of Medicine, Los Angeles, California 90024

R. Dwelle[b)] and P. Katzka[b)]

Litton Applied Technology, Sunnyvale, California 94086

(Received 30 April 1987; accepted for publication 29 July 1987)

A new method for rapidly acquiring fluorescence spectra from optical probes using an acousto-optic tunable filter (AOTF) has been developed. The AOTF consists of a piezoelectric transducer bonded to a birefringent crystal. Acoustic waves are generated in the crystal by an applied radio frequency. For a given radio frequency, only a narrow band of optical frequencies will be diffracted. Unlike normal Bragg diffraction which can only be used with collimated light, the AOTF has a large angular aperture (up to 28 deg) and can therefore be coupled to an uncollimated broadband white light source, photomultiplier tube, or camera. Using the device and a xenon–mercury arc lamp, excitation and emission spectra of the fluorescent *p*H probe BCECF were acquired in 17 ms (spectral resolution = 4 nm). Rapid wavelength switching or modulation of selected wavelengths was achieved at $\sim 10^5$ Hz. The device is also capable of spectral imaging with a spatial resolution of greater than 100 lines/mm.

INTRODUCTION

The use of optical probes to monitor intracellular ion concentrations in living cells is becoming increasingly popular in the field of cell biology.[1–3] Currently, fluorescent probes are available whose emission or excitation spectral properties vary in response to changes in intracellular *p*H (pH_i) or intracellular Ca^{2+} (Ca_i^{2+}).[1–3] Specifically, BCECF (pH_i probe) and FURA-2 (Ca_i^{2+} probe) have a shift in their excitation spectra so that the ratio of two fluorescent excitation wavelengths are used to quantitate pH_i or Ca_i^{2+}. 1,4-DHPN (pH_i probe) and INDO-1 (Ca_i^{2+} probe) have spectral shifts in their emission spectra. With these probes, the ratio of two fluorescent emission intensities are currently measured to quantitate pH_i or Ca_i^{2+}.

Previous methodology for rapidly acquiring spectral information from either endogenous or exogenous optical probes in living cells have utilized a monochromator coupled to either a diode array or a two-dimensional detector.[2,4–6] This methodology is useful for rapidly acquiring fluorescence emission or absorbance spectra yet is limited by expense and the inability to measure excitation spectra. These considerations prompted the development of a new technique for rapidly acquiring spectral information from optical probes using an acousto-optic tunable filter which is capable of acquiring emission, excitation, and absorbance spectra on a ms time scale. Because of its high spatial resolution (> 100 lines/mm), the AOTF can also be used for spectral imaging applications.

I. MATERIALS

The acousto-optic tunable filters were designed with two types of birefringent crystals which differed in their spectral properties. Tellurium oxide (TeO_2) is the preferred AOTF material due to its high acousto-optic figure of merit. This crystal, although useful in the visible and infrared region, cannot be utilized for ultraviolet applications due to its short-wavelength transmission cutoff at 360 nm. For ultraviolet spectroscopy, crystalline quartz is the preferred material. In the present study, the fluorescence and laser experiments utilized a TeO_2 noncollinear AOTF with a design angle of 25°. (Design angle refers to the angle between the incident light beam and the optical axis of the crystal.) The ulraviolet scan of the mercury arc lamp utilized a collinear quartz AOTF with a design angle of 101.6°. $LiNbO_3$ piezoelectric transducers were metal bonded to the crystals. Radio frequency power amplifiers (models 600 and 300) were purchased from ENI (Rochester, NY) and the sweep oscillator (model 2000) was purchased from Wavetech Indiana, Inc. (Beachgrove, IN). Arc lamps used in the present study were purchased from Oriel Corp. (Stamford, CT). Photomultiplier tubes were of the type RCA #7265 with an F20 cathode (RCA, Lancaster, PA). Spectra were displayed on either a 7834 storage oscilloscope (Tektronix, Beaverton, OR) or recorded on a 7132-A strip-chart recorder (Hewlett–Packard, Palo Alto, CA). The monochromator used in some experiments was a model 1870 (Spex Industries, Metuchen, NJ). The argon laser used to calibrate the TeO_2 tunable filter was model CR4 (Coherent, Inc., Palo Alto, CA). 2, 7-biscarboxyethyl-5,6-carboxyfluorescein (BCECF) was purchased from Molecular Probes, Inc. (Junction City, OR).

II. THEORY OF OPERATION

Acousto-optic devices consist of a piezoelectric transducer bonded to a crystal.[7] When the transducer is excited by an applied rf signal, acoustic waves are generated in the

 0034-6748/87/111996-08$01.30 © 1987 American Institute of Physics

This article is copyrighted as indicated in the article. Reuse of AIP content is subject to the terms at: http://scitationnew.aip.org/termsconditions. Downloaded to IP: 35.8.11.3 On: Wed, 27 Jan 2016 03:00:41

medium. The propagating acoustic waves produce a periodic modulation of the index of refraction via the elasto-optic effect.[8] This provides a moving phase grating which, under proper conditions, will diffract portions of an incident light beam. A simple acousto-optic device or Bragg cell can be used, in principle, as an electronically tuned optical filter.[9] However, such an optical filter is impractical, since its angular aperture is proportional to the spectral bandwidth and becomes exceedingly small for useful spectral resolutions. The small angular aperture feature of isotropic acousto-optic diffraction results from the fact that a change of the angle of the incident light will introduce a momentum mismatch and a corresponding decrease of diffraction efficiency [Fig. 1 (a)]. The angular aperture associated with acousto-optic diffraction in an isotropic medium is thus quite small. For an incident light beam of finite divergence, the width of the passband is greatly increased. Thus, in isotropic Bragg diffraction, the filtering action is extremely sensitive to the angle of incident light and is thus usable only with collimated light. In addition, the diffracted beam is deflected to a different angle for each wavelength, an effect similar to that produced by a prism.[9]

The filters designed for the present study are based on acousto-optic diffraction in an anisotropic medium (birefringent crystal).[10–13] In this type of filter, there are two loci of wave vectors (one each for the ordinary and extraordinary polarized light). The momentum of the light deflected (k_d) is no longer the same as that of the incident light (k_i):

$$k_i = 2\pi n_e/\lambda_0 \text{ and } k_d = 2\pi n_0/\lambda_0, \qquad (1)$$

where n_o and n_e are, respectively, the index of refraction for the ordinary and extraordinary wave in the birefringent medium and λ_0 is the passband wavelength. In the above equations, we are assuming that the light is polarized such that the incident light is an extraordinary ray. There are certain conditions where, in an anisotropic crystal, the momentum mismatch due to angular deviation of the incident light beam is negligible.[11–13] This concept is illustrated by the wave-vector diagram for acousto-optic diffraction in a uniaxial crystal where, referring to Fig. 1 (b), the acoustic wave vector is chosen so that the tangents to the incident and diffracted light wave vectors' surfaces are parallel. When these tangents are parallel, the acousto-optic diffraction becomes relatively insensitive to the angle of incident light, a process termed noncritical phase matching (NPM). The parallel tangents condition is met in a collinear AOTF,[11,12] where acousto-optic interaction involves optic and acoustic waves propagating collinearly in a plane perpendicular to the optic axis [Fig. 1 (b)]. Since the zero order and the diffracted beams are collinear, polarizers must be used to separate them in this type of filter.

Since the refractive indices for ordinary and extraordinary light in a birefringent crystal are not the same, it is possible to choose the direction of acoustic wave propagation so that the phase mismatch due to angular variation of light incidence is compensated by the angular change of birefringence and, hence, the NPM is maintained to first order over a large angular change of the incident light beam [Fig. 1(c)].[13] The parallel tangents condition implies that the

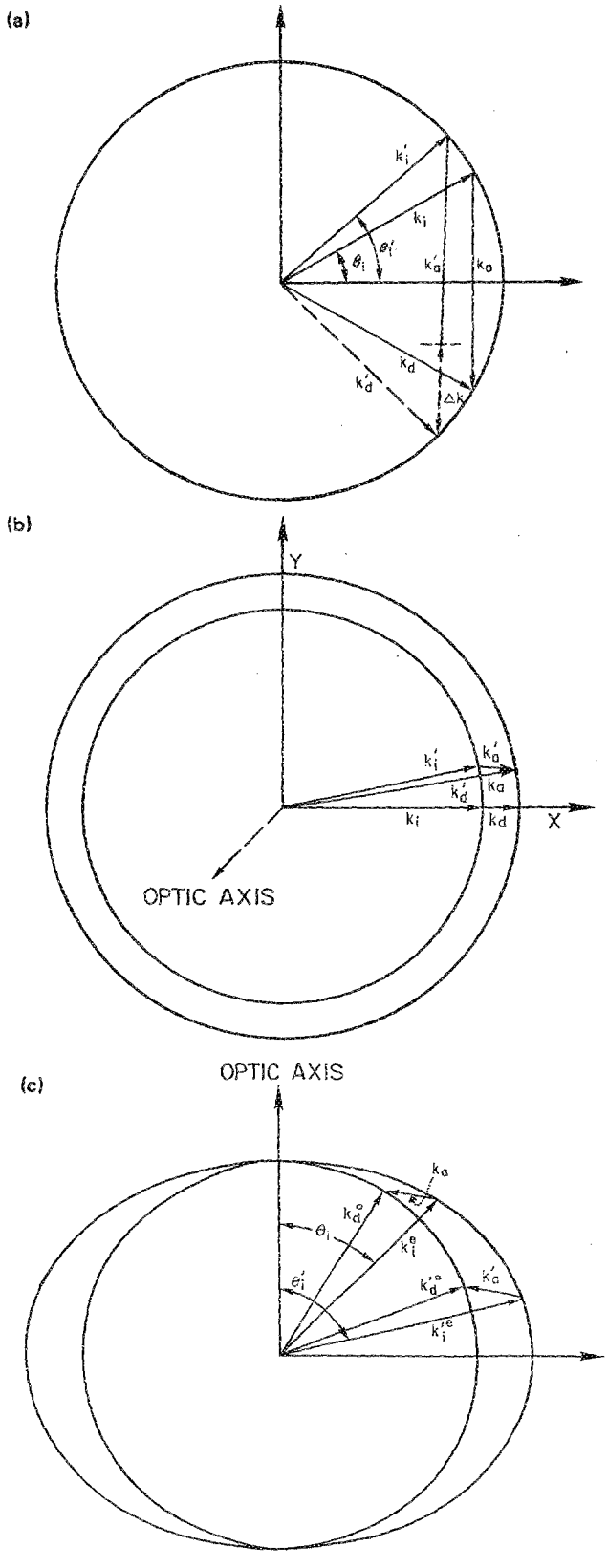

FIG. 1. (a) Wave-vector diagram for acousto-optic interaction in an isotropic crystal (Bragg cell). (b) Wave-vector diagram for acousto-optic interaction in an anisotropic crystal (collinear). The optic axis is perpendicular to the page. θ_i is measured between the optic axis and the x axis and is equal to 90°. (c) Wave-vector diagram for acousto-optic interaction in an anisotropic crystal (noncollinear). k_i, k_i' = momentum of incident light; k_a, k_a' = momentum of acoustic wave; k_d, k_d' = momentum of diffracted light; k_i^e, $k_i'^e$ = momentum of extraordinary incident light; and k_d^o, $k_d'^o$ = momentum of diffracted ordinary light.

This article is copyrighted as indicated in the article. Reuse of AIP content is subject to the terms at: http://scitationnew.aip.org/termsconditions. Downloaded to IP: 35.8.11.3 On: Wed, 27 Jan 2016 03:00:41

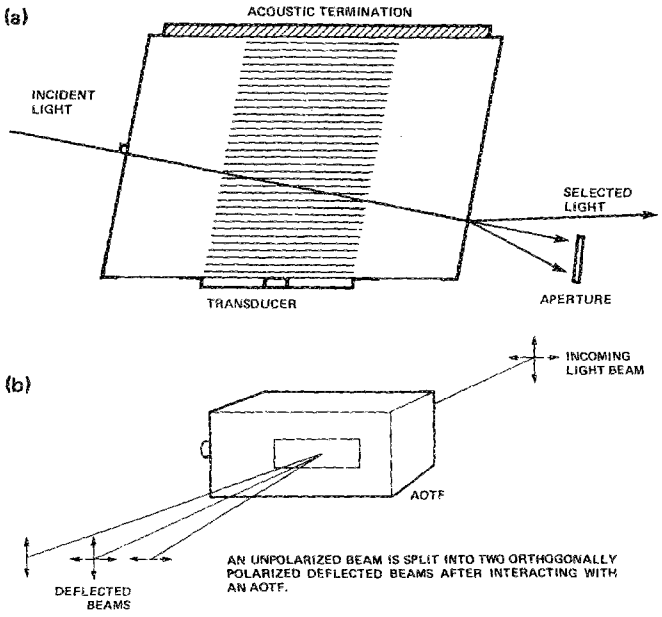

FIG. 2. (a), (b). Acousto-optic tunable filter (AOTF). The AOTF designed for the present study consisted of either a TeO_2 (tellurium oxide) crystal or crystalline quartz bonded to a piezoelectric transducer.

group velocity for the incident and diffracted light is collinear, and thus the two orthogonally polarized beams do not separate until they exit from the crystal, as shown in Figs. 2(a) and (b). An important advantage of this noncollinear AOTF is the first-order absence of change in angle of deflection with a change of wavelength. This implies that only a single fixed detector is necessary during a spectral scan. In addition, this type of filter can be operated without polarizers.

The passband wavelength (λ_0) of a birefringent AOTF filter is related to the acoustic frequency (f_a) by

$$\lambda_0 = (\Delta n/f_a)k, \tag{2}$$

where k is a design parameter and Δn is the birefringence of the crystal. Since Δn varies with wavelength, λ_0 and f_a are not exactly inversely related (Figs. 3 and 4).

Under phase matching conditions, the diffracted light intensity grows along the interaction length. The peak transmission (T_0) is given by the ratio of the intensity of diffracted light to that of incident light.

$$T_0 = \sin^2\left(\frac{\pi^2}{2}\frac{\bar{M}_2}{\lambda_0^2}P_d L^2\right)^{1/2}, \tag{3}$$

where P_d is the acoustic power density, $\bar{M}_2$ is a normalized acousto-optic figure of merit, and L is the interaction length. Assuming constant acoustic power density, the phase-matched light intensity increases approximately as the square of the interaction length for collinear AOTFs and directly for noncollinear AOTFs.

The spectral resolution $\Delta\lambda$ of the AOTF is given by

$$\Delta\lambda = (\lambda_0^2/L)/k, \tag{4}$$

where again k is a factor dependent on the AOTF design. For a noncollinear AOTF, the incident light beam and the diffracted light beam are separated spatially. From the simple wave vector for acousto-optic diffraction, one can show that the angle between the incident and diffracted beam is approximately given by

$$\Delta\phi = \Delta n \sin\Theta_i. \tag{5}$$

For a collinear crystal, $\Theta_i = 90°$ and $\Delta\phi = 0$.

III. RESULTS

A. Rapid scanning optical spectroscopy

The characteristics of the two types of birefringent tunable filters utilized in the present study are listed in Table I.

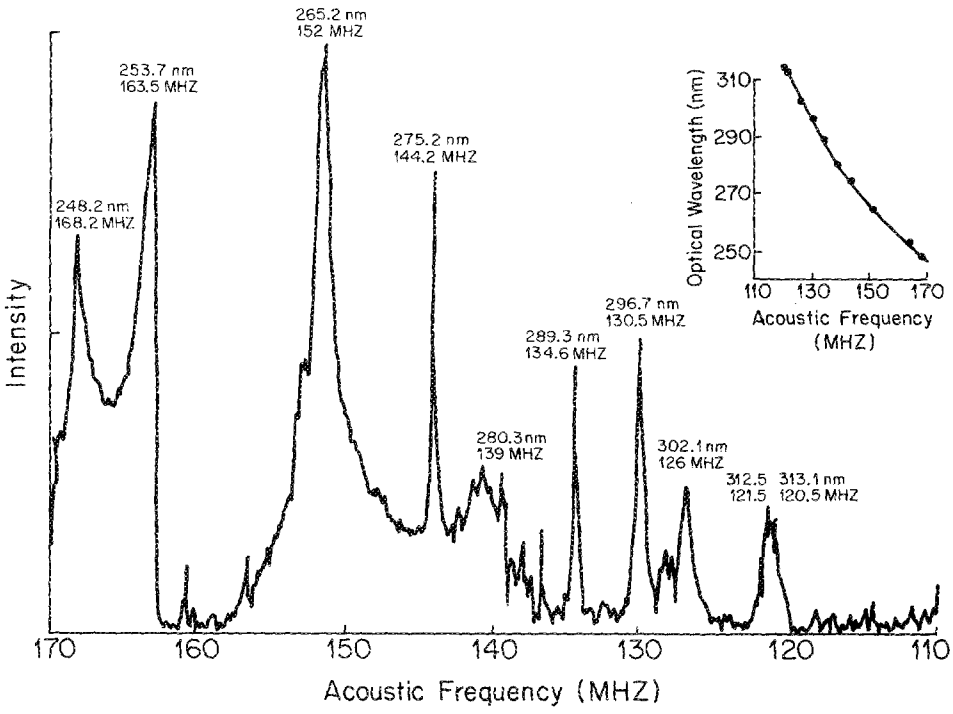

FIG. 3. Ultraviolet spectrum of a 150-W mercury arc lamp scanned with the quartz AOTF. The spectral resolution is 0.09 nm at 325 nm. Scan time was ~10 s. Insert: Calibration of applied acoustic frequency vs optical wavelength. The peaks of the mercury arc lamp were utilized to calibrate the quartz AOTF.

This article is copyrighted as indicated in the article. Reuse of AIP content is subject to the terms at: http://scitationnew.aip.org/termsconditions. Downloaded to IP: 35.8.11.3 On: Wed, 27 Jan 2016 03:00:41

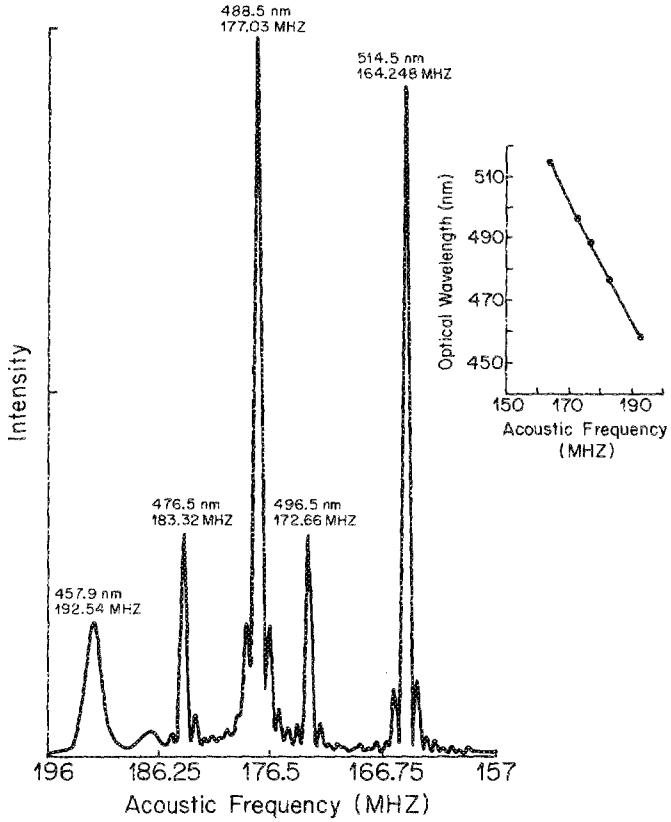

FIG. 4. Spectral output of an argon-ion laser scanned with the TeO_2 AOTF. The spectral resolution was 1.7 nm at 488.5 nm. Scan time ~2 s. Insert: Calibration of applied acoustic frequency vs optical wavelength. The peaks of the argon laser were utilized to calibrate the AOTF.

TABLE I. AOTF characteristics.

	TeO_2	Quartz
1 Design angle	25°	101.6°
2 Dimensions	8×10×15 mm	10×10 mm×10 cm
3 Optical aperture	3×5 mm	7×7 mm
4 Acceptance angle	4.5°	5°
5 Spectral resolution	1.7 nm at 488.5 nm	0.09 nm at 325 nm[a]
6 Optical tuning range	360–700 nm	250–400 nm
7 Corresponding drive frequency	270–125 MHz	163–94 MHz
8 Random access	6 μs	16 μs
9 Maximum modulation frequency (full on, full off)	200–250 kHz	50 kHz
10 Efficiency	400 nm 98% (0.3-W drive power)	325 nm 85% (10-W drive power)
11 (a) peak/1st sidelobe no apodization	13 dB	13 dB
with apodization	30 dB	30 dB
(b) peak/background rejection	60 dB[b]	30 dB[c]
12 Temperature-induced wavelength drift	0.05 nm/°C	0.008 nm/°C

[a] Measured with a helium–cadmium laser.
[b] Limited by optical scatter in the bulk material and optical surfaces.
[c] Limited by cross polarizer rejection.

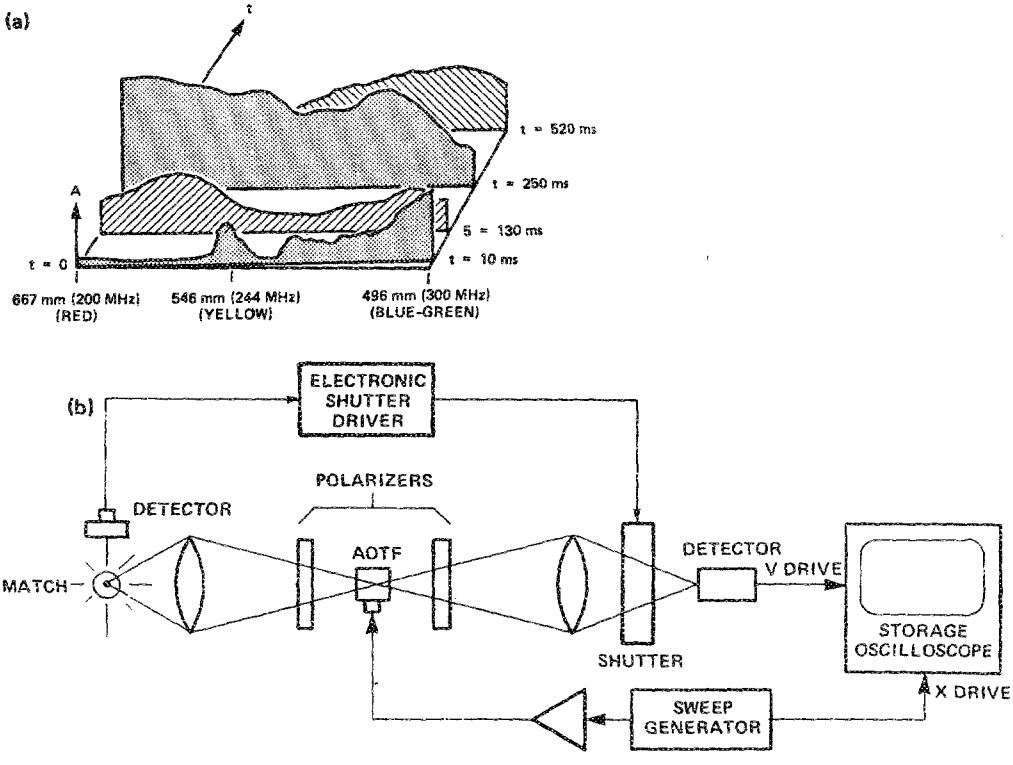

FIG. 5. (a) Selected time resolved spectra of an igniting match head. (b) Block diagram.

This article is copyrighted as indicated in the article. Reuse of AIP content is subject to the terms at: http://scitationnew.aip.org/termsconditions. Downloaded to IP: 35.8.11.3 On: Wed, 27 Jan 2016 03:09:41

Since a given acoustic frequency will diffract only a narrow band of optical wavelengths [Eqs. (1) and (2)], and the diffracted beam is deflected to the same angle for each wavelength, optical spectra can be acquired by scanning the radio frequency. The optical spectrum of a 150-W mercury arc lamp acquired with the collinear quartz AOTF is depicted in Fig. 3. The spectral resolution at 325 nm was 0.01 nm; scan time ~ 10 s.

The spectrum of a multiline argon laser is depicted in Fig. 4. The spectrum was acquired in ~ 2 s with the TeO_2 AOTF. The spectral resolution at 488.5 nm was 1.7 nm. The AOTF has a spectral bandpass whose profile is the square of the Fourier transform of the acoustic profile along the light path. For the unapodized AOTF used in this experiment, this instrumental function is the sinc^2 response. Apodizing the acoustic profile would result in a sizable reduction in the first sidelobes (Table I).[14] Spectra can be acquired for kinetic applications as demonstrated in Figs. 5(a) and 5(b) which show the optical spectral characteristics of an igniting match acquired in the first 0.5 s following ignition. The ability to rapidly scan an uncollimated light source [Figs. 3, 5(a), and 5(b)] makes the device ideally suited for rapidly acquiring fluorescent spectra from optical probes.

Figure 6(a) depicts a block diagram of a fluorometer designed with two AOTFs for rapid scanning spectroscopy. Figure 6(b) illustrates a fluorescent excitation (452–518 nm) spectrum of 10-μM BCECF in a Hepes buffered solution, pH 7.4. The spectrum was obtained by scanning the AOTF (TeO_2) in front of a 150-W xenon–mercury arc lamp. The excitation wavelengths were focused onto a cuvette containing the dye. The emission intensity was monitored with a second AOTF (TeO_2) tuned to 528 nm which was coupled to a photomultiplier tube. The duration of the scan was 17 ms. By scanning the AOTF in front of the photomultiplier tube (from 498 to 548 nm) and tuning the excitation AOTF to 498 nm, the emission spectrum depicted in

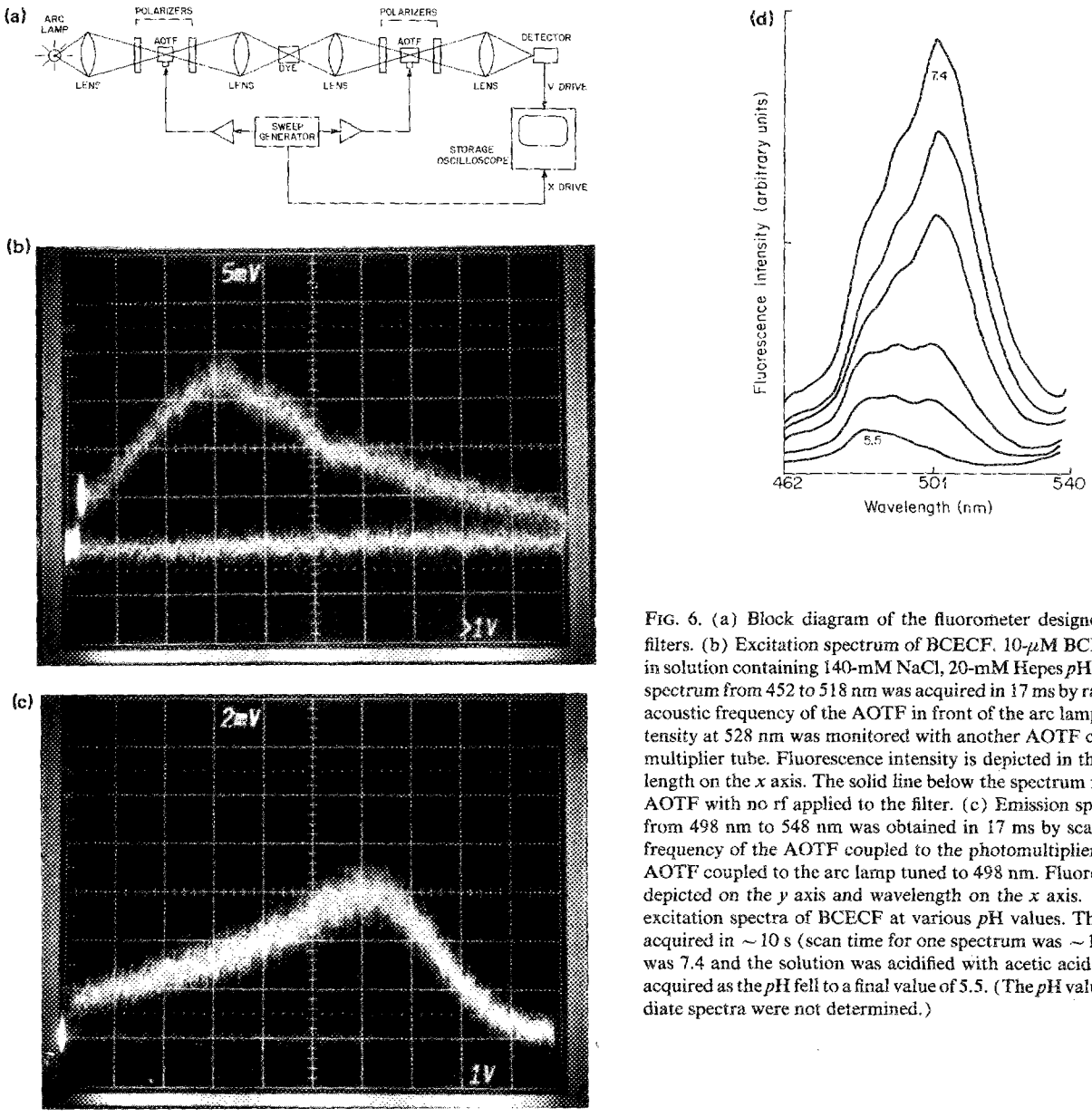

FIG. 6. (a) Block diagram of the fluorometer designed with two TeO_2 filters. (b) Excitation spectrum of BCECF. 10-μM BCECF was dissolved in solution containing 140-mM NaCl, 20-mM Hepes pH 7.4. The excitation spectrum from 452 to 518 nm was acquired in 17 ms by rapidly scanning the acoustic frequency of the AOTF in front of the arc lamp. The emission intensity at 528 nm was monitored with another AOTF coupled to a photomultiplier tube. Fluorescence intensity is depicted in the y axis and wavelength on the x axis. The solid line below the spectrum is the output of the AOTF with no rf applied to the filter. (c) Emission spectrum of BCECF from 498 nm to 548 nm was obtained in 17 ms by scanning the acoustic frequency of the AOTF coupled to the photomultiplier tube, keeping the AOTF coupled to the arc lamp tuned to 498 nm. Fluorescence intensity is depicted on the y axis and wavelength on the x axis. (d) Time resolved excitation spectra of BCECF at various pH values. The six spectra were acquired in ~ 10 s (scan time for one spectrum was ~ 1 s). The initial pH was 7.4 and the solution was acidified with acetic acid. The spectra were acquired as the pH fell to a final value of 5.5. (The pH values for the intermediate spectra were not determined.)

This article is copyrighted as indicated in the article. Reuse of AIP content is subject to the terms at: http://scitationnew.aip.org/termsconditions. Downloaded to IP: 35.8.11.3 On: Wed, 27 Jan 2016 03:00:41

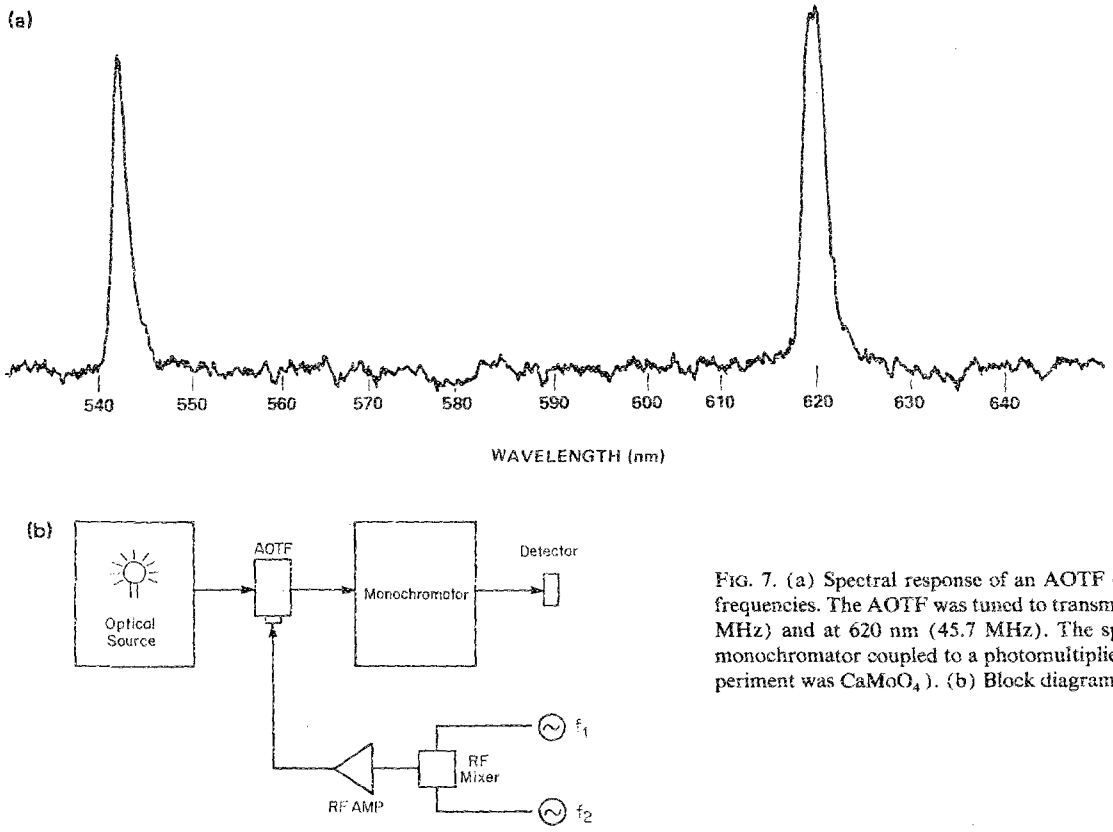

FIG. 7. (a) Spectral response of an AOTF driven simultaneously at two frequencies. The AOTF was tuned to transmit maximally at 542 nm (59.4 MHz) and at 620 nm (45.7 MHz). The spectrum was detected with a monochromator coupled to a photomultiplier tube (the crystal in this experiment was $CaMoO_4$). (b) Block diagram.

Fig. 6 (c) was acquired in 17 ms. The ability to collect fluorescent spectra kinetically is depicted in Fig. 6(d), which illustrates an experiment in which six excitation spectra of the *p*H dye BCECF were acquired in the first 10 s following acidification of the solution containing the dye.

In the experiments depicted in Figs. 6 (a)–6(d), the spectral output of the arc lamp and the spectral sensitivity of the photomultiplier tube were not corrected for. However, by varying the acoustic power density during a scan at the appropriate acoustic frequencies, it is possible to correct for the spectral output of the excitation source and the spectral sensitivity of the detector (photomultiplier tube or two-dimensional detector). This ability to electronically alter the spectral shape of the output of the filter is depicted in Fig. 7. In this experiment, two oscillators were utilized to drive the crystal at two separate radio frequencies. The resultant transmission spectrum has a peak at 542 and 620 nm.

IV. WAVELENGTH RATIOING

When acquiring kinetic data from pH_i and Ca_i^{2+} probes, it is not always necessary to acquire spectral information continually. It is often sufficient to monitor the ratio of two excitation or emission wavelengths only. Since dye

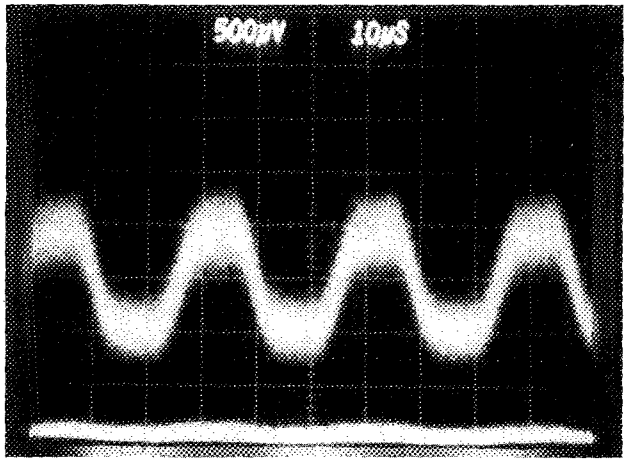

FIG. 8. Rapid alternation between two excitation wavelengths 440 nm/500 nm at 167 kHz. The trace depicts the photomultiplier tube output. The peak represents 500 nm, the trough 440 nm.

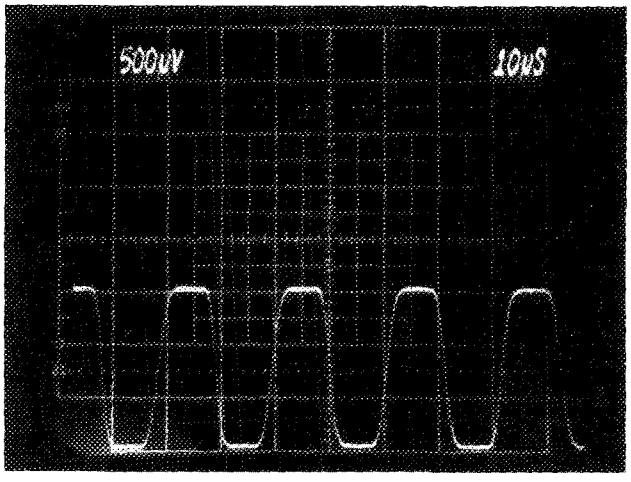

FIG. 9. Modulation of a single wavelength 540 nm at 250 kHz.

This article is copyrighted as indicated in the article. Reuse of AIP content is subject to the terms at: http://scitationnew.aip.org/termsconditions. Downloaded to IP: 35.8.11.3 On: Wed, 27 Jan 2016 03:00:41

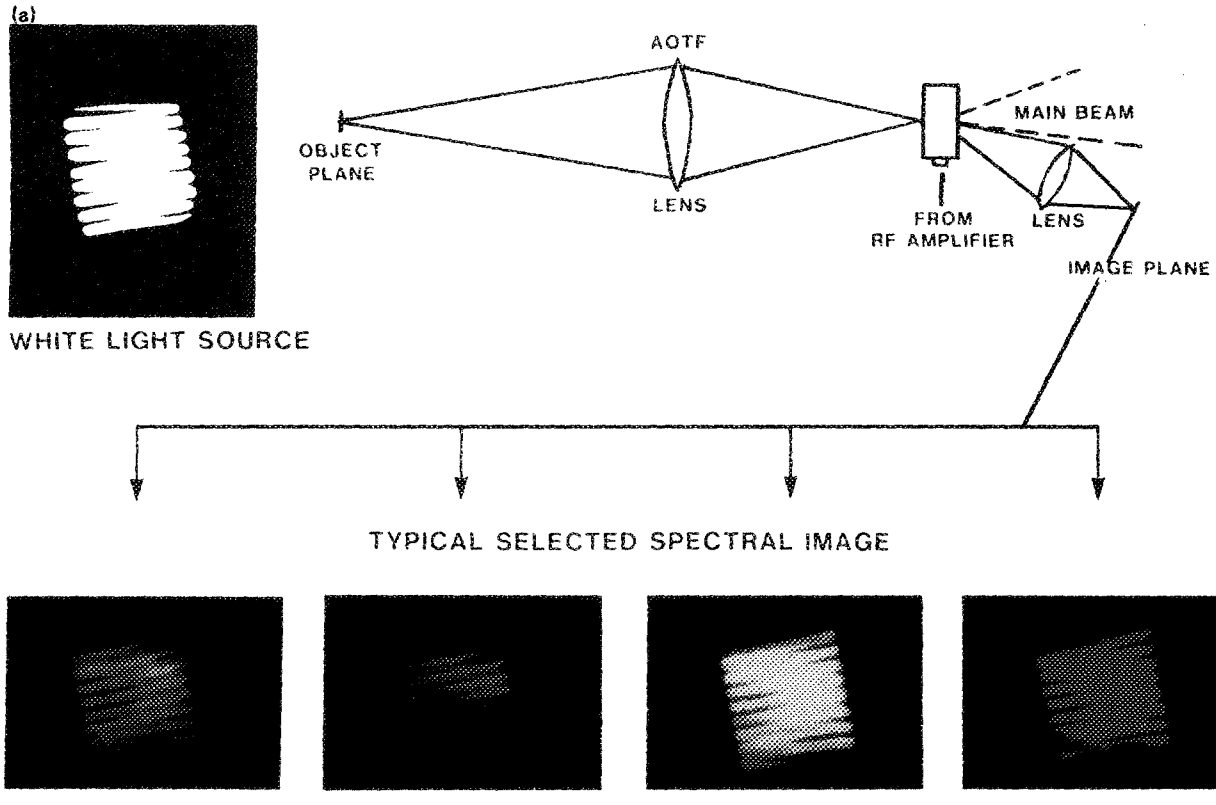

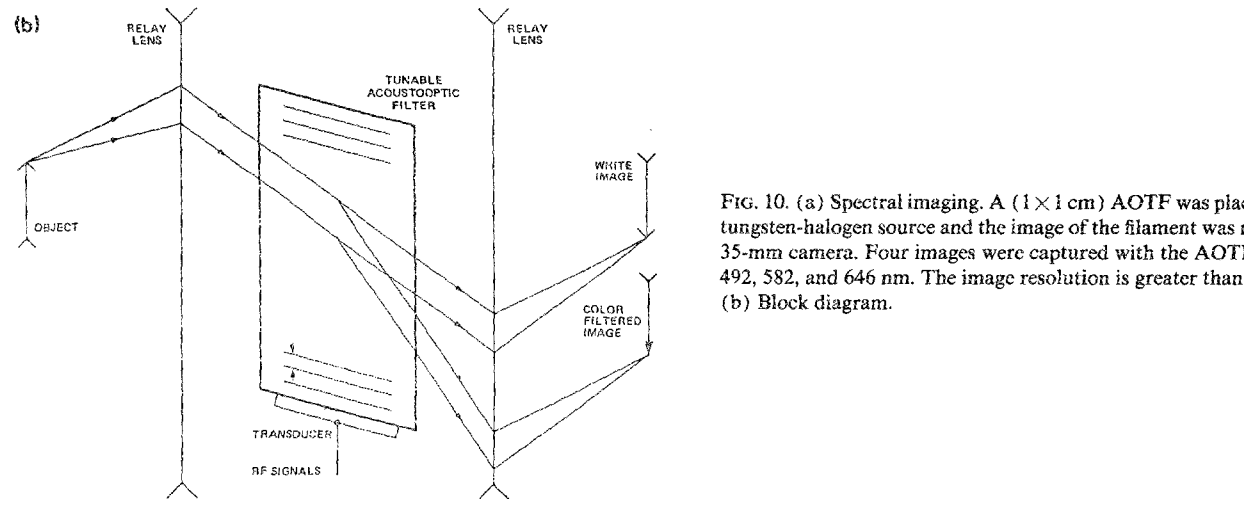

FIG. 10. (a) Spectral imaging. A (1 × 1 cm) AOTF was placed in front of a tungsten-halogen source and the image of the filament was recorded with a 35-mm camera. Four images were captured with the AOTF tuned to 450, 492, 582, and 646 nm. The image resolution is greater than 100 lines/mm. (b) Block diagram.

leakage and bleaching will decrease the fluorescent intensity at the two wavelengths (especially in single cell experiments), it is essential to alternate between the two wavelengths as rapidly as possible. For this application, the peak transmission of the AOTF was alternated between the two excitation wavelengths, 440 and 500 nm (for BCECF) at 167 kHz (Fig. 8). This alternation rate is adequate for single cell fluorescent applications. We have recently described another technique for rapidly acquiring fluoroscence excitation ratios by modulating two excitation wavelengths simultaneously and using two lock-in amplifiers to demodulate the fluorescent emission intensity into its two components.[15] A single AOTF, however, could be used (as a multiwavelength modulator) by coupling the AOTF to a broadband source and tuning the transmission spectrum of the filter so that it transmits only at two excitation wavelengths, e.g., 440 and 500 nm, for BCECF (as in Fig. 7). Simultaneously, each wavelength could be modulated electronically at different frequencies and two lock-in amplifiers would be used to demodulate the fluorescent emission into its two components. An example of single wavelength modulation at 250 kHz (540 nm) is depicted in Fig. 9.

V. SPECTRAL IMAGING

Recently, spectral imaging has been used to acquire spatial and spectral information from fluorescent probes in single cells.[16,17] The AOTF can be operated near the focal plane for a multispectral imaging application as shown in Figs. 10(a) and 10(b). To demonstrate this capability, a tungsten-halogen lamp filament was imaged onto the TeO_2 AOTF and the diffracted beam was reimaged onto a 35-mm camera. Four images of the lamp filament were acquired at 450, 492, 582, and 646 nm. The image resolution was greater

This article is copyrighted as indicated in the article. Reuse of AIP content is subject to the terms at: http://scitationnew.aip.org/termsconditions. Downloaded to IP: 35.8.11.3 On: Wed, 27 Jan 2016 03:00:41

than 100 lines/mm. The AOTF, when coupled to a microfluorometer, will therefore be able to be used to measure spatial maps of pH_i or Ca_i^{2+} with fluorescent probes in living cells (ratio imaging at two wavelengths). The rapidity with which the AOTF can alternate between two spectral images, $\sim 10^5$ Hz, far exceeds the framing rate of most television cameras (33 Hz) at the present time. With the development of more rapid scanning cameras, this will be less of a limitation.

VI. CONCLUDING REMARKS

The acousto-optic tunable filters designed for the present study are all solid-state optical filters that operate on the principle of acousto-optic interaction in a birefringent crystal.[10–13] The spectral bandpass of the filter can be tuned or rapidly programmed over a large portion of the optical region, simply by changing the frequency of the applied electrical signal. Thus, the AOTF functions as an electrically tuned optical filter. The large angular aperture is most significant since it provides a throughput advantage compared to a grating monochromator. It also allows the AOTF to be operated near the focal plane for multispectral imaging applications. This, however, is not its only advantage. The AOTF can be operated in sequential or random wavelength access and multiwavelength modes. The device can also be amplitude and wavelength (FM) modulated, and due to its electronic input, it is relatively easy to interface to a microcomputer. It is anticipated that the new techniques described in the present report will likely have widespread and as yet unforeseen applications in the fields of cell biology, astronomy, chemistry, and physics.

ACKNOWLEDGMENTS

This research was supported by Grant R23 AM36324 from the National Institute of Health, and Grant 4197 from the Academic Senate, UCLA, Los Angeles Division (all to IK).

[a] Address correspondence to: Ira Kurtz, M.D., Division of Nephrology, Department of Medicine, UCLA School of Medicine, Los Angeles, CA 90024.

[b] Present address: AOTF Technology, Sunnyvale, CA 94086.

[1] T. J. Rink, R. Y. Tsien, and T. Pozzan, J. Cell. Biol. **95**, 189 (1982).

[2] I. Kurtz and R. S. Balaban, Biophys. J. **48**, 449 (1985).

[3] G. Grynkiewicz, M. Poenie, and R. Y. Tsien, J. Biol. Chem. **260**, 3440 (1985).

[4] E. Kohen, C. Kohen, J. M. Salmon, G. Bengtsson, and B. Thorell, Biochem. Biophys. Acta. **263**, 575 (1974).

[5] L. J. Mandel, T. G. Riddle, and J. C. Lammana, in *Oxygen and Physiological Function*, edited by F. Jobsis (Professional Library, Dallas, TX, 1976), pp. 79–89.

[6] R. S. Balaban, I. Kurtz, H. E. Cascio, and P. A. Smith, J. Microsc. **141**, 31 (1986).

[7] I. C. Chang, IEEE Trans. Sonics Ultrason. **SU-23**, 2 (1976).

[8] M. Born and E. Wolf, in *Principles of Optics*, 3rd ed. (Pergamon, New York, 1965), Chap. 2.

[9] A. H. Rosenthal, J. Opt. Soc. Am. **45**,751 (1955).

[10] R. W. Dixon, IEEE J. Quantum Electron. **QE-3**, 85 (1967).

[11] S. E. Harris and R. W. Wallace, J. Opt. Soc. Am. **59**, 744 (1969).

[12] J. A. Kusters, D. A. Wilson, and D. L. Hammond, J. Opt. Soc. Am. **64**, 434 (1974).

[13] I. C. Chang, Appl. Phys. Lett. **25**, 370 (1974).

[14] I. C. Chang, P. Katzka, J. Jacob, and S. Estrin, IEEE Ultrason. Symp. Proc., 40 (1979).

[15] I. Kurtz, J. Clin. Invest. (1987 in press).

[16] L. Tanasugarn, P. McNeil, G. T. Reynolds, and D. L. Taylor, J. Cell. Biol. **98**, 717 (1984).

[17] D. A. Williams, K. E. Fogarty, R. Y. Tsien, and F. S. Fay, Nature **318**, 558 (1985).

This article is copyrighted as indicated in the article. Reuse of AIP content is subject to the terms at: http://scitationnew.aip.org/termsconditions. Downloaded to IP: 35.8.11.3 On: Wed, 27 Jan 2016 03:09:41